First high dynamic range and high resolution images of the sky obtained with a diffractive Fresnel array telescope

Laurent Koechlin · Jean-Pierre Rivet · Paul Deba · Denis Serre · Truswin Raksasataya · René Gili · Jules David

Abstract This paper presents high contrast images of sky sources, obtained from the ground with a novel optical concept: Fresnel arrays. We demonstrate the efficiency of a small 20 cm prototype Fresnel array for making images with high brightness ratios, achieving contrasts up to 4×10^5 on sky sources such as Mars and its satellites, and the Sirius A–B couple. These validation results are promising for future applications in space, for example the 4 m array we have proposed to ESA in the frame of the "Call for a Medium-size mission opportunity for a launch in 2022". Fresnel imagers are the subject of a topical issue of Experimental Astronomy published in 2011, but only preliminary results were presented at the time. Making images of astronomical bodies requires an optical component to focus light. This component is usually a mirror or a lens, the quality of which is critical for sharp and high contrast images. However, reflection on a mirror and refraction through a lens are not the only ways to focus light: an alternative is provided by diffraction through binary masks (opaque foils with multiple precisely etched sub-apertures). Our Fresnel arrays are such diffractive focusers, they offer weight, price and size advantages over traditional optics in space-based astronomical instruments. This novel approach requires only void apertures of special shapes in an

L. Koechlin (✉) · P. Deba · T. Raksasataya · J. David
Institut de Recherches, en Astrophysique et Planétologie (IRAP), Université de Toulouse, CNRS, 14 Avenue Edouard Belin, 31400 Toulouse, France
e-mail: laurent.koechlin@ast.obs-mip.fr

J.-P. Rivet · R. Gili
Observatoire de la Côte d'Azur, Laboratoire Cassiopée, Université de Nice Sophia-Antipolis, CNRS, BP 4229, 06304 Nice Cedex 04, France

D. Serre
Leiden Observatory, Leiden University, P.O. Box 9513, 2300RA Leiden, The Netherlands

opaque material to form sharp images, thus avoiding the wavefront distortion, diffusion and spectral absorption associated with traditional optical media. In our setup, lenses and/or mirrors are involved only downstream (at small sizes) for focal instrumentation and chromatic correction. Fresnel arrays produce high contrast images, the resolution of which reaches the theoretical limit of diffraction. Unlike mirrors, they do not require high precision polishing or positioning, and can be used in a large domain of wavelengths from far IR to far UV, enabling the study of many science cases in astrophysics from exoplanet surfaces and atmospheres to galaxy evolution.

1 Introduction

For the visible or near IR domains, two main kinds of space telescope have been considered for space operation: solid aperture or "mosaic" designs such as NASA's James Webb Space Telescope [9], and long-baseline "diluted aperture" interferometers, such as TPF-I, Darwin and related projects [22]. Solid aperture instruments will eventually be limited in diameter, hence in sensitivity and resolution, because of technical and financial constraints (relating to the surface accuracy of large traditional optics, and to their weight). Long-baseline interferometers in the visible or IR domains are limited to fields $< 0.1''$ [17], and their operation in space requires formation flying of several telescopes at micrometrical precision over large distances [21, 27].

In this article, we present the first *high resolution* and *high dynamic range* images of sky objects obtained with diffractive focusing devices, inherited from the historical "Fresnel zone plate" [8, 31]. The principle is to use diffraction through a mask to focus light, instead of refraction through a lens or reflection on a mirror. Our diffracting mask is a set of alternatively transmissive and opaque zones, the transmissive zones being arc-shaped holes in an opaque foil. The positions and shapes of these void arcs are precisely computed to guarantee constructive interferences at some distance f on the optical axis. For a chosen wavelength λ_c, the central radius R_k of each arc follows the corresponding circle of rank k in a Fresnel zone plate:

$$R_k = \sqrt{2\lambda_c f (k + \alpha - 1) + \lambda_c^2 (k + \alpha - 1)^2} \ . \tag{1}$$

In the above expression, α is a phase shift at center, determining the radius and nature (i.e. opaque or void) of the first zone.

For a Fresnel zone-plate having $k_{\max}$ zones and a diameter $\Phi = 2R_{k_{\max}}$, the focal length f depends on the actual observation wavelength λ:

$$f \approx \frac{\Phi^2}{8\,k_{\max}\,\lambda} \tag{2}$$

As a result of dependance on λ, the raw image of a Fresnel zone plate is highly chromatic. We introduce a diffractive corrector after prime focus, to achieve broad band achromatic imaging [29]. The point spread function of our Fresnel array has also been optimized for high contrast by square aperture apodization [23]. At present we modulate the arcs widths to vary light transmission in the aperture plane. In the future, modulating the arcs displacements could add some control on the phase variation across the aperture, contributing to phase induced amplitude apodization [12].

Unlike historical Fresnel zone plates, our Fresnel arrays have no optical substrate; the diffracting structure of concentric arcs that form the Fresnel zones is laser-carved into a thin foil. To support the rings without a substrate and minimize overall light scattering, we mathematically superpose a slimmed orthogonal Fresnel mesh on them [28]. The result is a set of closed circuits with arcs of Fresnel rings and straight segments. Each time a circuit is completed by a laser tool, a small chip is removed from the foil, leaving a precisely chiseled aperture. Our 20 × 20 cm arrays have 696 Fresnel-zones and approximately 700,000 apertures. A previous occurrence of "open" Fresnel zone plate was designed by Baez [2], with 19-zones supported by four radial struts, for X-ray imaging.

Several proposals have been made in the recent years for using Fresnel zone plates in space, held by, or painted on transparent plastic foils: [3, 4, 6, 15], but these proposals have never been implemented successfully. Others for making images in the X-ray domain, now also for UV and visible wavelengths, propose diffraction through circular holes: "photon sieves" [1, 16]. However, their point spread functions have side lobes that are not well suited for high dynamic range imaging.

One characteristic of diffractive focusing is its strong chromatic aberration, linked to a variation of the focal length as a function of wavelength. The Fresnel array acts like a grating, and this chromatic aberration has to be cancelled. Otherwise, the usable spectral band would be so reduced that it would affect the sensitivity and scope of the instrument. To overcome this diffraction-induced chromatic aberration, we use a second diffraction that cancels the first one [7, 32]: a small divergent Fresnel lens is placed in a pupil plane, where our field optics produce a small image of the 20 × 20 cm main Fresnel array. Both diffractive elements have the same number of Fresnel zones, and lie in optically conjugated planes. The small, secondary Fresnel lens is blazed, and operates at diffraction order −1.

We have tested our Fresnel arrays for high dynamic range imaging on broad spectral bands, both in laboratory and on the sky. The concept, potential applications, preliminary studies and preliminary results are published in a topical issue of Experimental Astronomy [5, 11, 14, 20, 20, 24–26, 29, 30].

The validation results presented here are the best ones to date, obtained with the nominal test-bed on high contrast binary stars and various sky objects. In the following sections, we shortly describe the test-bed and how we assessed its performance. We conclude by presenting some science cases that could be addressed by a future space mission.

2 The test-bed

With the Centre National d'Etudes Spatiales (CNES) in 2009, we carried out a study for a Fresnel imager space mission. We ran numerical simulations and tests to validate the optical concept. A first series of laboratory tests followed, yielding high resolution imaging with 10^6 dynamic ranges [28, 29]. The on-sky tests we report on in this article were made with a new test-bed, as described in [26] and [19]. The primary array is carved by a UV laser machine tool into a cooper foil, 50 μm thick. We have also tested images made by Fresnel arrays carved into black plastic foils and into layered foils of copper and polyimides, both provide good stability and are promising for folding and unfolding in large dimension applications. Our test-bed (sketched in Fig. 1) uses two separate modules to simulate a two-satellite architecture. The first one holds a 20×20 cm square Fresnel array, the second module 18m downstream is placed at the primary focal plane. It holds the field optics, chromatic correction and detectors.

For the ground-based prototype, we attached the Fresnel array and the secondary module respectively to each end of a long telescope, as described
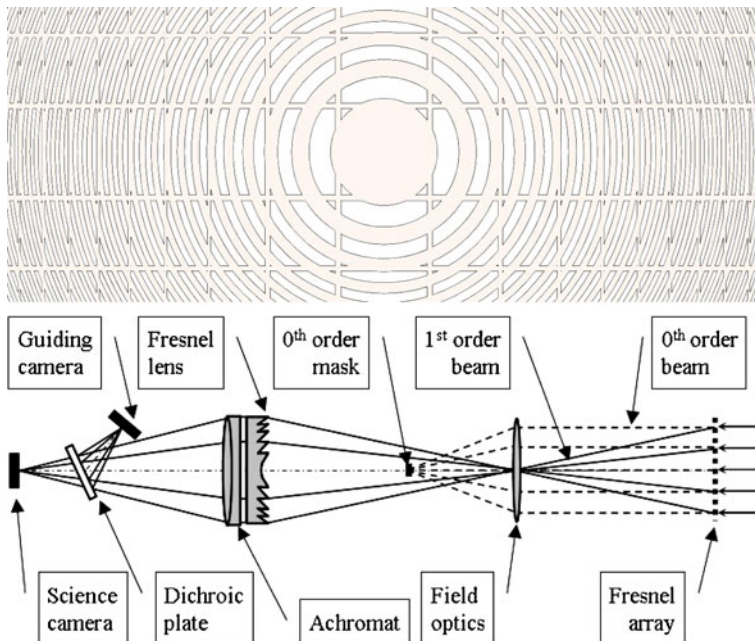

Fig. 1 *Top*: Fresnel array, close view on the central zones. *Bottom*: sketch of our prototype, *not to scale* for clarity. On the real prototype, the Fresnel lens and the achromat doublet are much smaller than the entrance Fresnel array. The distance between the Fresnel array and the field optics is 18 m. The rest of the light path is short (2 m). The zero-order mask blocks the light that has not been focused by the Fresnel array: all diffraction orders are blocked, except one. The achromat forms the final image after chromatic correction by the secondary Fresnel lens
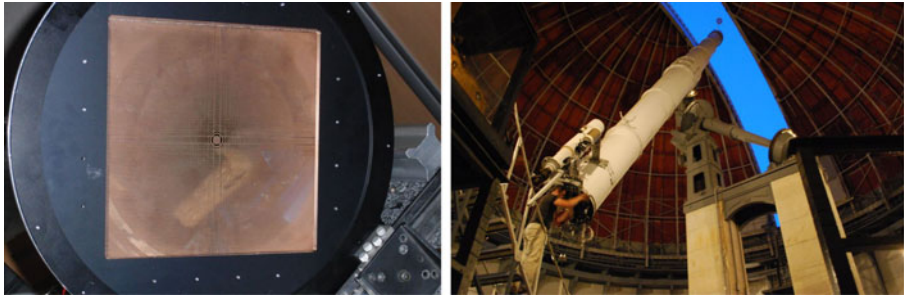
Fig. 2 *Left*: the 20 × 20 cm, 696-zone square Fresnel array in its cell. *Right*: picture taken by one of the authors (D.S.) showing the test-bed fitted aside the 19 m long refractor's tube at Observatoire de Nice. The Fresnel array is visible against the sky, held on a stem above the far side of the telescope. The optical bench holding the secondary module is visible at the near side of the telescope, just above the head of the person working on it (J-P.R.)

in [26] and [19]. We used the 76 cm aperture refractor at Observatoire de Nice (Fig. 2). The telescope optics are not used here: the optical axis of our prototype runs in free air, parallel to the 19 m long tube. Perching our optical elements high above ground and using this large instrument built in 1886 has been part of the challenge, but thanks to the high quality of its mount and the active maintenance policy at Observatoire de la côte d'azur, the drive has the high precision required for our purposes. The good quality of the seeing above and inside the large dome (built by Eiffel) has also been an advantage for achieving diffraction limited resolution with a 20 cm aperture.

3 On-sky results

3.1 Angular resolution and field

The aberration-free field of a 700-zone Fresnel array such as ours could reach 1.5°. On the test-bed, however, it is limited to 9′ (arc minutes) by the field optics aperture: 4.5 cm. Indeed, to maintain a cost advantage compared to a classical space telescope, the field optics mirror should remain small compared to the size of the main aperture Fresnel array. The long focal length thus limits the angular field. A space imager featuring a 6m primary Fresnel array and a 1m diameter field optics mirror, operated in the UV at 180 nm wavelength, would allow fields of 15″ (and yield angular resolutions of 6 milliarcseconds). To assess both the field capabilities and the angular resolution with our test-bed, we took images of the Moon (Fig. 3) and stellar sky sources such as ϵ Lyr (Fig. 4 left). The diagonal of the sensor covers 7.9′. We also obtained images of a diffuse and wide-field source : the central region of M42 (Fig. 4 right). The details visible on these images are compatible with the nominal diffraction-limited resolution of a 20 cm square aperture at 800 nm (0.8″).
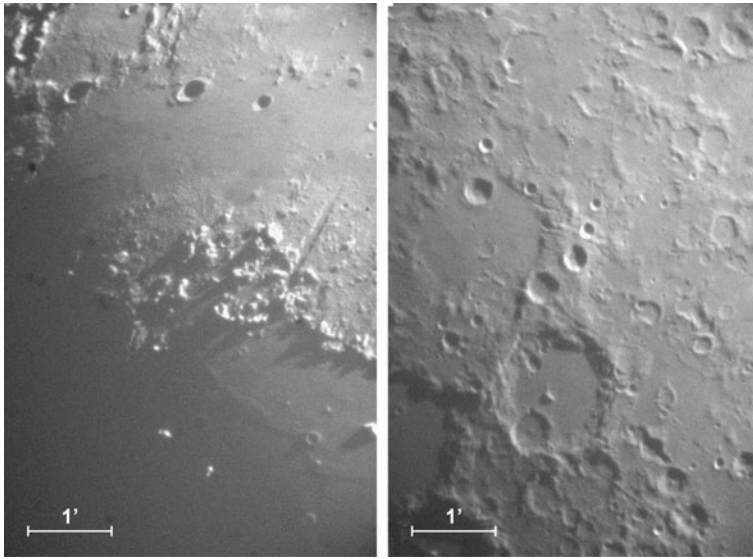
Fig. 3 Snapshots of the surface of the moon at first quarter, made with the 20×20 cm diffractive Fresnel imager in the spectral domain 745 to 840 nm, 2011-05-10 at 19h UT. *Left*: *Vallis Alpes* near the terminator. *Right*: *Hipparchus Crater*. Both images are $4.4' \times 6.6'$. They are slightly cropped

3.2 Dynamic range

3.2.1 Sirius A–B

We have tested the dynamic range on high contrast astronomical objects (a faint source close to a bright one). To estimate the achievable brightness ratio, we chose Sirius A (α CMa), a bright main sequence star around which orbits a white dwarf companion: Sirius B (Fig. 5). In the optical setup, a secondary Fresnel lens is placed after focus for dispersion correction. This small diffractive lens is blazed for 800 nm, but with Sirius we chose to use the $630 - 740$ nm spectral band rather than the nominal $745 - 840$ nm wavelength setting. At the nominal (close IR) setting, the brightness ratio between Sirius B and A is less favorable, due to the temperature difference between these stars, and we could not detect the companion. At the alternate wavelength setting ($630 - 740$ nm), the companion has been detected with a *signal/noise* ratio of 5, and a brightness ratio between Sirius B and A of $5.6 \ 10^{-5}$. Their measured separation and orientation are in agreement with the WDS catalogue: respectively $8.6''$ and $+92, 5°$.

Our EMCCD camera (Andor Luca s) is not adapted to very high contrast images, due to small but systematic and level dependant background irregularities. We had to smooth out these irregularities by letting the stars slowly drift during acquisition and record a series of short exposure frames (83 ms), then recenter them by *"shift and add"*. The *Python* code that we developed
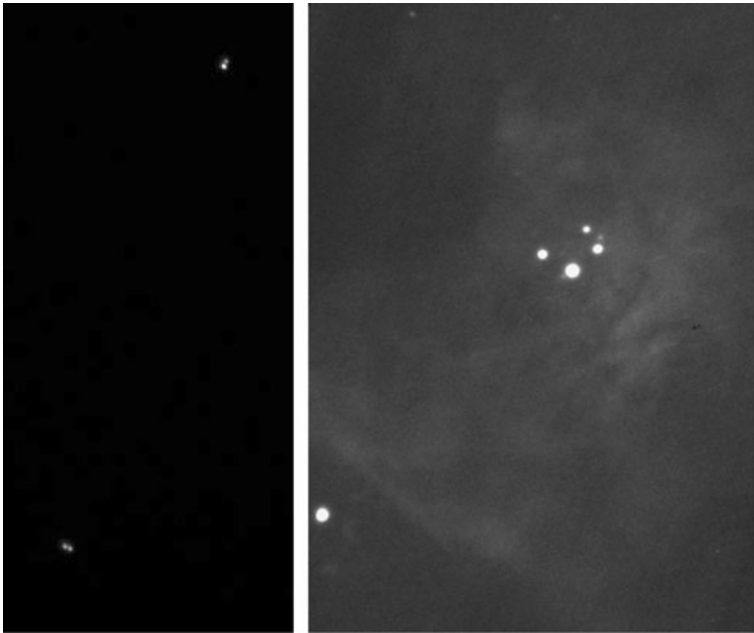
Fig. 4 *Left*: broad-band exposure on the "double-double" star ϵ Lyr. The A and B components are in the *upper-right* corner, with 2.53″ separation and V magnitudes 4.67 and 6.10. The C and D components are in the *lower-left* corner, with 2.34″ separation and V magnitudes 5.25 and 5.38. *Right*: central region of M42 nebula in Orion imaged with an H-α (650 − 662 nm) bandpass filter. One can see the four main stars of the θ Ori stellar system (the trapezium), in addition to fainter ones and the nebula in the background. In these pictures, north is up, east right

for this purpose is publicly available upon request. In the case of Sirius A–B only, an additional post-processing step has been required: the subtraction of a reference star (not deconvolution). We used Procyon (β CMi) as a reference source for a point spread function of the optics. This star is not a perfect point source as it has a white dwarf companion too, but it could be used as a reference in our case, being given its close separation and high brightness ratio.

3.2.2 Mars satellites

To test the dynamic range in the vicinity of a bright and extended object, we made images of Phobos and Deimos: the boulder-shaped satellites orbiting close to Mars, having mean diameters of 22 and 12 km; Mars has a diameter of 6,794 km. The brightness ratio between Mars and its satellites is estimated to 240,000 and 680,000, respectively. Postprocessing steps have been added to the reduction pipeline for these images of Mars and its satellites. A set of time-averaged images have been computed from series of 200 frames, 1s exposure time each. In the individual frames, Mars disc's is overexposed and just used for recentering. This procedure has been repeated at roughly 5 min intervals for
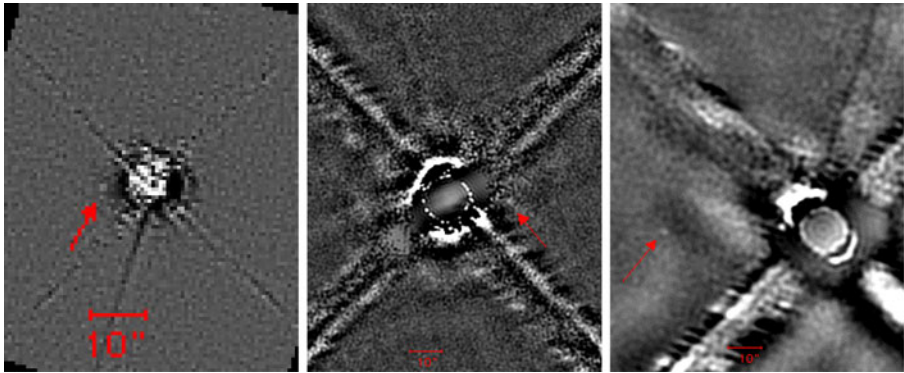
Fig. 5 High contrast sky objects by the 20×20 cm diffractive Fresnel imager. North is up, east right. The spikes are artifacts coming from the diffraction of light on the slimmed orthogonal Fresnel mesh superimposed to hold mechanically the Fresnel rings. *Left*: Sirius AB couple, $630 - 740$ nm spectral band. The companion Sirius B appears as a small dot on the East at $8.6''$. The light of Sirius A saturates the display over a few diffraction radii. *Middle*: Mars satellite Phobos, 2010-02-13 at 00h07 UT, *Right*: Deimos, 2010-02-14 at 22h49 UT. The image of Mars is saturated

an hour, yielding a 13 frames film of the satellites' rotation around Mars. The satellites are detectable at that point, but barely because a spatial modulation of the background remains, due to residual noise from the camera and stray light in the optics. So we subtracted an average of the whole film to each of its images. Then, low-pass filtering is applied to remove spurious structures smaller than the diffraction-limited resolution limit. Two of the best images in the films are shown Fig. 5 middle and right.

To our knowledge, the smallest instrument to image the satellites of Mars previously was a 30 cm mirror telescope. With our prototype, we have shown that a smaller (20×20 cm) diffractive array can do it. This does not mean that classical optics could not reach equivalent performances, but it proves the suitability of diffractive focusing for high resolution and high contrast imaging.

4 Conclusion and science perspectives

On a small 20×20 cm prototype, we have validated a novel optical concept for astronomical imaging. The resolution and dynamic range attained are promising for a large space borne instrument. Potentially, this concept is well fitted for space missions in any spectral domain, from far UV (100 nm) to IR (25 μm). However, the advantages of Fresnel arrays become outstanding in the UV domain, for which a 6 m size aperture yields milliarcseconds angular resolutions with a very rough manufacturing precision compared to standard optics: typically 50 μm compared to 10 nm.

Fresnel arrays of 6 m and larger have focal lengths of a few kilometers in the UV; they will require two satellites flying in formation around Lagrangian point $L2$, but with tolerant positioning in translation (a few centimeters).

Orbits, operation modes, tolerances and mass budgets have been precisely studied for the ESA proposal we submitted. The most stringent positioning constraint is the orientation of the secondary module, pointing to the center of the primary. A misalignment leads to linear dispersion in the image field, such as with an objective prism. Indeed, the combination of two Fresnel diffractions of equal power and opposite orders yields a plane wavefront, which is tilted when one Fresnel zone plate is displaced with regard to the optical axis of the other. The result is the same as what would be obtained with a uniformly spaced, plane grating, the period of this virtual grating being inversely proportional to the relative displacement of the zone plates. This can be voluntarily set for low spectral resolution observation of sparse fields, like with a grism instrument such as WFC3 (in grism modes) on HST. For achromatic and diffraction limited imaging, the tolerance in attitude depends on the spectral bandpass: the larger the bandpass, the more stringent the alignment. For example, one gets an orientation tolerance of $\sim 0.1''$ for a 6 m aperture configuration operating in a broad spectral band with $\Delta\lambda/\lambda = 0.25$ centered on the Lyman-α wavelength. Very broad bandpasses such as "IR to UV" would require very large field optics, potentially larger than the main aperture, thus financially inadequate. Such large bandpasses can be sampled by a Fresnel imager, however sequentially.

Concerning angular resolution, a Fresnel array behaves quasi-identically to a solid aperture of the same size, but a thin foil is much lighter and less bulky (when folded) than a mirror. Concerning collecting power, it is proportional to the square of its aperture as with a mirror, but the photometric throughput reaches only 6 to 8%. However, this drawback should be compensated by the availability of a larger aperture size for a Fresnel array based system, at equal or lower price than a standard mirror based telescope, for large apertures.

4.1 Science cases

Our initial drive for developing this concept providing a high quality of wavefront was to study exoplanets [18], but there are many other fields of astrophysics that could benefit from imaging with angular resolutions of a few milliarcseconds and very high contrasts. We present some examples.

4.1.1 Asteroids and planets of our solar system

Many carbon-based molecules suspected to be present in the atmospheres of planets in our solar system have numerous UV lines; the high angular resolution of a large Fresnel array would allow a detailed study of the asteroids size, shape, and chemical composition, that would be a good complement to the studies planned by the GAIA mission [13, 33]: the high dynamic range reached should reveal a few hundred new binary asteroids, allowing measurement of masses and internal densities. Development of a 6 m class instrument with spectro-imaging capabilities also leads to a precise study of the atmospheres and soil composition of larger planets and satellites. The

milliarcsecond angular resolution would provide sampling scales of 2 km on Mars at opposition, and 20 km on Jupiter, for example.

4.1.2 Accretion disks around young stars

At longer distances, there is established scientific interest in the UV domain for the accretion disks around young stars and formation of exoplanetary systems [10, 11, 25]. These rotating reservoirs of gas and dust are the birthplaces of new planetary systems and UV radiation plays an important role in synthesizing the organic molecules necessary for the emergence of life.

4.1.3 UV scattering in galaxies

In galaxy physics and cosmology [24], a Fresnel array operating in the UV could assess the scattering processes in close-by, but also distant galaxies (up to $Z = 2$) that are seen with insufficient spatial resolution from ground based telescopes or from HST. Precise knowledge on this first link would strengthen the cosmology models at large scales.

The science cases presented above are just a sample of what could be done with a 6 m foil. With a larger Fresnel array $(10 - 15\,m)$, angular resolutions and fields would become competitive over a broad range of wavelengths, no longer restricted to UV, expanding the scope to new science cases such as telluric exoplanet study.

4.1.4 Exoplanets

According to numerical simulations published in Koechlin et al. [18], the study with enough spectral resolution of a telluric exoplanet at 10 parsecs orbiting a solar-type star in the habitable zone is feasible with a Fresnel array, but would require apertures of 15 m to 40 m, and a 6 m aperture is required for a Jovian exoplanet. We have not compared in depth the performances with starshade configurations or other coronagraphic techniques. A space mission that involves formation flying and new optical concepts such as ours is more challenging than classical ones, so to improve our chances of being selected one day by a space agency there is a tradeoff in budget, which limits the aperture size.

This is why we propose studies in the UV domain, where we think we have an advantage at small aperture over classical optics. Of course larger Fresnel arrays are even more promising, and fitted to a broad range of wavelengths and science cases.

still operational more than 125 years later for testing future space projects such as ours. Special thanks to C. Evans-Pughe and Clive Coen for their help with the text.

References

1. Andersen, G.: Large optical photon sieve. Opt. Lett. **30**, 2976–2978 (2005)
2. Baez, A.: Fresnel zone plate for optical image formation using extreme ultraviolet and soft x radiation. J. Opt. Soc. Am. **51**(4), 405–412 (1961)
3. Barton, I.M., et al.: Fabrication of large-aperture lightweight diffractive lenses for use in space. Appl. Opt. **40**, 447–451 (2001)
4. Chesnokov, Y.M.: A space-based very high angular resolution telescope. Russ. Space Bull. **1**, 18–21 (1993)
5. Deba, P., Etcheto, P., Duchon P.: Preparing the way to space borne Fresnel imagers: space scenarios optical layouts. Exp. Astron. **30**(2–3), 123–136 (2010). doi:10.1007/s10686-010-9202-5
6. Early, J.T.: Large space telescopes using Fresnel lens for power beaming, astronomy and sail missions. In: Beamed Energy Propulsion: First International Symposium on Beamed Energy Propulsion, AIP Conference Proceeding, vol. 664, pp. 399–410 (2003)
7. Faklis, D., Morris, G.M.: Broadband imaging with holographic lenses. Opt. Eng. **28**(6), 592–598 (1989)
8. Fresnel, A.: Mémoire sur la diffraction de la lumière. Archives des sciences physiques et naturelles, académie des sciences, Paris. Tome **V**, 339–475 (1818)
9. Gardner, J.P., et al.: The James Webb space telescope. Space Sci. Rev. **123**, 485–606 (2006). doi:10.1007/s11214-006-8315-7
10. Gomez de Castro, A.-I., Lecavelier, A., D'Avillez, M., Linsky, J.L., Cernicharo, J.: UV capabilities to probe the formation of planetary systems: from the ISM to planets. ApSS **303**, 33–52 (2006)
11. Gomez de Castro, A.I.: The Fresnel space imager as a disk evolution watcher. Exp. Astron. **30**(2–3), 205–216 (2011). doi:10.1007/s10686-011-9223-8
12. Guyon, O.: Phase-induced amplitude apodization of telescope pupils for extrasolar terrestrial planet imaging. Astron. Astrophys. **404**, 379–387 (2003)
13. Hestroffer, D., dellŌOro, A., Cellino, A., Tanga, P.: The Gaia mission and the asteroids. Lect. Notes Phys. **790**, 251–340 (2010). doi:10.1007/978-3-642-04458-86
14. Hinglais, E.: A space Fresnel imager concept assessment study led by CNES for astrophysical applications. Exp. Astron. **30**(2–3), 85–110 (2011). doi:10.1007/s10686-011-9218-5
15. Hyde, R.A.: Eyeglass. 1. Very large aperture diffractive telescopes. Appl. Opt. **38**, 4198–4212 (1999)
16. Kipp, L., et al.: Sharper images by focusing soft X-rays with photon sieves. Nature **414**, 184–188 (2001)
17. Koechlin, L., Perez, J-P.: A limit in Field-resolution ratio for interferometric arrays. In: Traub, W. (ed.) Interferometry for Optical Astronomy, II. SPIE Proc., vol. 4838, pp. 411–415. Hawaii (2002)
18. Koechlin, L., Serre, D., Duchon, P.: High resolution imaging with Fresnel interferometric arrays: suitability for exoplanet detection. Astron. Astrophys. **443**, 709–720 (2005)
19. Koechlin, L., Rivet, J.-P., Gomez de Castro, A.I.: Fresnel arrays and their astrophysical applications. Exp. Astron. **30**(2–3), 83–84 (2011). doi:10.1007/s10686-011-9225-6
20. Koechlin, L., et al.: Generation 2 testbed of Fresnel imager: first results on the sky. Exp. Astron. **30**(2–3), 165–182 (2011). doi:10.1007/s10686-010-9203-4
21. Martin, S.R., et al.: A midinfrared nuller for terrestrial planet finder: design, progress, and results. In: Coulter, D.R. (ed.) Techniques and Instrumentation for Detection of Exoplanets. SPIE Proc., vol. 5170, pp. 144–154 (2003)
22. Mennesson, B., Leger, A., Ollivier, M.: Direct detection and characterization of extrasolar planets: the Mariotti space interferometer. Icarus **178**(2), 570–588 (2005). doi:10.1016/j.icarus.2005.05.012
23. Nisenson, P., Papaliolios, C.: Detection of earth-like planets using apodized telescopes. Astrophys. J. **548**, L201–L205 (2001)

24. Pello, R., Maizy, A., Richard, J.: Extragalactic science with the FRESNEL imager. Exp. Astron. **30**(2–3), 195–204 (2011). doi:10.1007/s10686-010-9206-1
25. Raksasataya, T., Gomez de Castro, A.I., Koechlin, L., Rivet, J.-P.: A space Fresnel imager for ultra-violet astrophysics: example on accretion disks. Exp. Astron. **30**(2–3), 183–194 (2011). doi:10.1007/s10686-011-9221-x
26. Rivet, J.-P., Koechlin, L., Raksasataya, T., Deba, P., Gili, R.: Fresnel imager testbeds: setting up, evolution and first images. Exp. Astron. **30**(2–3), 149–164 (2011). doi:10.1007/s10686-011-9213-x
27. Shao, M., Catanzarite, J., Pan, X.: The synergy of direct imaging and astrometry for orbit determination of exo-earths. Astroph. J. **720**, 357 (2010)
28. Serre, D., Deba, P., Koechlin, L.: Fresnel interferometric imager: ground-based prototype. Appl. Opt. **48**(15), 2811–2820 (2009)
29. Serre, D.: The Fresnel imager: instrument numerical model. Exp. Astron. **30**(2–3), 111–121 (2011). doi:10.1007/s10686-010-9200-7
30. Serre, D., Koechlin, L., Deba, P.: The Fresnel imager: learning from ground-based generation I prototype. Exp. Astron. **30**(2–3), 137–147 (2010). doi:10.1007/s10686-010-9201-6
31. Soret, J.-L.: Sur les phénomènes de diffraction produits par les réseaux circulaires. Arch. Sci. Phys. Nat. **52**, 320–337 (1875)
32. Schupmann, L.: Die medial-fernrohre: eine neue konstruktion f–r grosse astronomische instrumente. Teubner B G (1899)
33. Tanga, P., Hestroffer, D., Delbo, M., Richardson, D.C.: Asteroid rotation and shapes from numerical simulations of gravitational re-accumulation. Planet. Space Sci. **57**, 193–200 (2009). doi:10.1016/j.pss.2008.06.016